High Glycolate Oxidase Activity Is Required for Survival of Maize in Normal Air[1][OA]

Israel Zelitch*, Neil P. Schultes, Richard B. Peterson, Patrick Brown, and Thomas P. Brutnell

Department of Biochemistry and Genetics, The Connecticut Agricultural Experiment Station, New Haven, Connecticut 06511 (I.Z., N.P.S., R.B.P.); and Department of Plant Biology (P.B.) and Boyce Thompson Institute for Plant Research (T.P.B.), Cornell University, Ithaca, New York 14853

A mutant in the maize (*Zea mays*) *Glycolate Oxidase1* (*GO1*) gene was characterized to investigate the role of photorespiration in C_4 photosynthesis. An *Activator*-induced allele of *GO1* conditioned a seedling lethal phenotype when homozygous and had 5% to 10% of wild-type GO activity. Growth of seedlings in high CO_2 (1%–5%) was sufficient to rescue the mutant phenotype. Upon transfer to normal air, the *go1* mutant became necrotic within 7 d and plants died within 15 d. Providing [1-^{14}C]glycolate to leaf tissue of *go1* mutants in darkness confirmed that the substrate is inefficiently converted to $^{14}CO_2$, but both wild-type and GO-deficient mutant seedlings metabolized [1-^{14}C]glycine similarly to produce [^{14}C]serine and $^{14}CO_2$ in a 1:1 ratio, suggesting that the photorespiratory pathway is otherwise normal in the mutant. The net CO_2 assimilation rate in wild-type leaves was only slightly inhibited in 50% O_2 in high light but decreased rapidly and linearly with time in leaves with low GO. When *go1* mutants were shifted from high CO_2 to air in light, they accumulated glycolate linearly for 6 h to levels 7-fold higher than wild type and 11-fold higher after 25 h. These studies show that C_4 photosynthesis in maize is dependent on photorespiration throughout seedling development and support the view that the carbon oxidation pathway evolved to prevent accumulation of toxic glycolate.

The oxidation of glycolate to glyoxylate in higher plants is catalyzed by glycolate oxidase (GO; EC 1.1.3.15), an FMN-containing protein (Zelitch and Ochoa, 1953). The enzyme is located in the peroxisome and performs an essential step in the operation of the oxidative photorespiratory cycle accompanying photosynthetic CO_2 assimilation in C_3 plants (Tolbert, 1971, 1997). Glycolate arises from 2-phosphoglycolate, which is produced together with 3-phosphoglycerate by ribulose bisphosphate reacting with O_2 as catalyzed by Rubisco (Bowes et al., 1971; Ogren, 2006) in the bundle sheath (BS) cell of C_4 plants (Edwards and Walker, 1983). Dephosphorylation of 2-phosphoglycolate yields glycolate that is transported into the peroxisome. In the peroxisome, GO oxidizes glycolate to produce glyoxylate. Transamination of glyoxylate generates Gly that is converted to Ser and CO_2 in the mitochondrion (Tolbert, 1971). The Ser gives rise to glyceric acid, which is ultimately converted to 3-phosphoglyceric acid in the mesophyll (M) cell chloroplast (Usuda and Edwards, 1980). Thus, the photorespiratory pathway (Fig. 1) is a futile process that diverts energy to refixation of photorespired CO_2, thereby lowering the quantum efficiency of net carbon assimilation (Zelitch, 2001).

In C_3 leaves, production of photorespiratory CO_2 decreases net CO_2 assimilation by about 25% at 25°C, and photorespiration increases greatly relative to CO_2 assimilation at higher temperatures (Peterson, 1983; Hanson and Peterson, 1986). In C_4 plants such as maize (*Zea mays*), a carbon shuttle increases local CO_2 concentrations in the BS chloroplasts, where Rubisco is located, to levels more than three times higher than those found in M cells of C_3 plants. As a result, photorespiration is greatly reduced in C_4 tissues (Hatch, 1971; Jenkins et al., 1989; Dai et al., 1993; Laisk and Edwards, 1998).

Several studies point to a low, yet finite, rate of photorespiration in maize. To estimate photorespiration in maize leaves, Zelitch (1973) compared the initial rate of glycolate accumulation in leaf tissue in high light in the presence of an inhibitor of GO, α-hydroxysulfonate, and found that glycolate accumulation was 10% as great in maize as in tobacco (*Nicotiana tabacum*; C_3). Because no mechanism for the metabolism of glycolate is known without its first being converted to glyoxylate, this demonstrated that the rate of CO_2 production by photorespiration was no more than 5% of the net CO_2 assimilation rate (A) in C_4 photosynthesis. Additional studies that monitored $^{18}O_2$ and $^{13}CO_2$ exchange and estimates from electron transport suggested a similar photorespiratory rate in maize of 2% to 7% of A (Volk and Jackson, 1972; de Veau and Burris, 1989; Laisk and Edwards, 1998). Experiments with maize leaves in high light showed that with increasing O_2 level, there was

[1] This work was supported by the Hatch Fund (grant no. CONH00246 to R.B.P.) and by the National Science Foundation (grant no. DBI–0076892) to T.P.B.

* Corresponding author; e-mail israel.zelitch@po.state.ct.us.

The author responsible for distribution of materials integral to the findings presented in this article in accordance with the policy described in the Instructions for Authors (www.plantphysiol.org) is: Israel Zelitch (israel.zelitch@po.state.ct.us).

[OA] Open Access articles can be viewed online without a subscription.

www.plantphysiol.org/cgi/doi/10.1104/pp.108.128439

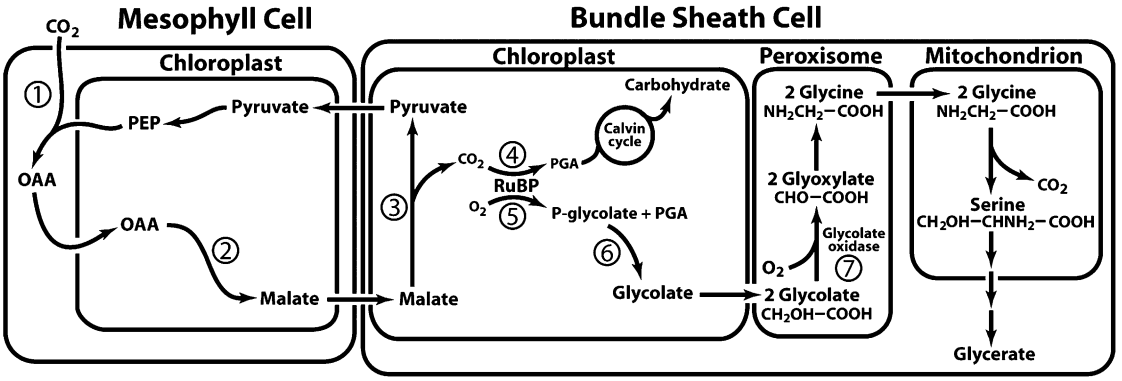

Figure 1. Schematic diagram of C_4 photosynthetic CO_2 assimilation in maize. The incoming atmospheric CO_2 reacts (1) with phospho*enol*pyruvate (PEP) to form oxaloacetate (OAA) in the M cell. The OAA is reduced (2) to malate through the NADP-malate dehydrogenase reaction, and the malate is converted to pyruvate and CO_2 by the NADP-malic enzyme (3) in the chloroplasts of BS cells. The released CO_2 combines with ribulose bisphosphate (RuBP) through the Rubisco reaction (4) to form phosphoglycerate (PGA). The resulting elevated CO_2 level inhibits, but does not eliminate, the oxygenase reaction (5) of Rubisco. Photorespiratory products are likely generated from incomplete suppression of Rubisco oxygenase activity in BS chloroplasts. A specific phosphatase in the chloroplast (6) converts the resulting P-glycolate to glycolate. The glycolate is transported to the peroxisome where GO activity (7), when present at high levels, creates glyoxylate. A series of aminotransferase and decarboxylation reactions leads to the production of Gly and Ser with the release of photorespiratory CO_2. Note that two Gly combine to produce one Ser and one CO_2. When GO activity is low or absent, the glycolate, which has no other means of being metabolized, will accumulate at rates equal to the rate of P-glycolate formation. For further details, refer to the introduction.

some decrease in *A*, and in limiting light a decrease in the maximum quantum yield was observed, further indicating that some photorespiration occurred (Dai et al., 1993).

A number of conditional mutants with lesions in different steps of the photorespiratory pathway were first obtained by Ogren and coworkers in Arabidopsis (*Arabidopsis thaliana*; Ogren, 1984, 2006) and later by others in barley (*Hordeum vulgare*; Blackwell et al., 1988) and tobacco (McHale et al., 1988). In these studies, mutants were identified that could survive in high CO_2, when photorespiration was blocked, but succumbed in normal air. Indeed, analyses of metabolite accumulation in these mutants provided biochemical evidence for a photorespiratory cycle (for review, see Reumann and Weber, 2006). However, no mutant lacking GO was ever recovered by this method of selection. The presence of five distinct *GO* loci in the Arabidopsis genome likely accounts for the failure to recover conditional *GO* mutants in previous screens.

Transgenic tobacco plants were generated that had reduced GO activity through cosuppression of the endogenous GO (Yamaguchi and Nishimura, 2000). These plants contained variable levels of GO activity that decreased during plant development, with some plants ultimately having as little as 20% of wild-type activity. Transgenic plants with greatly reduced levels of GO exhibited dramatically reduced photosynthetic electron transport rates in high light, whereas plants with moderate levels of GO were less affected.

In this report, we describe the isolation and characterization of a maize *GO* mutant caused by an *Activator* (*Ac*) insertion in *GO1* (*go1-m1*::*Ac*). Using *Ac* as a molecular tag, the *GO* gene was cloned and sequenced. In addition, mutant seedlings were characterized under both high and low CO_2 conditions. Under high CO_2 conditions, GO deficiency had no visibly adverse effects on plant growth. However, *A* was rapidly and linearly diminished in mutants in high light and high O_2. When such mutant plants were transferred from growth in high CO_2 to normal air in the light, glycolate accumulated linearly for 6 h to levels 7-fold greater than the initial concentration. Plants greatly depleted in GO activity were nonviable when grown at ambient CO_2 concentrations. We therefore conclude that photorespiration plays a vital role in C_4 photosynthesis.

RESULTS

Identifying a Maize *GO* Mutant

The *GO* mutant was first identified in sandbench screens of *Ac*-mutagenized families (Kolkman et al., 2005). A single family was identified that segregated a seedling lethal phenotype in 21 of the 71 seedlings examined, suggesting that the mutation was due to disruption of a single gene ($\chi^2 = 0.23$; $P = 0.63$). DNA-blot analysis was used to identify an *Ac*-containing, 3.2-kb *Eco*RI fragment that cosegregated with the mutant phenotype (data not shown). Approximately 800 bp of DNA flanking this sequence was recovered using an inverse PCR technique as described in "Materials and Methods." To recover additional sequences flanking the *Ac* insertion, we exploited the somatic instability of the active *Ac* insertion to selectively amplify *Ac* junction fragments that were generated through local insertions. This method, known as *Ac* casting (Singh et al., 2003),

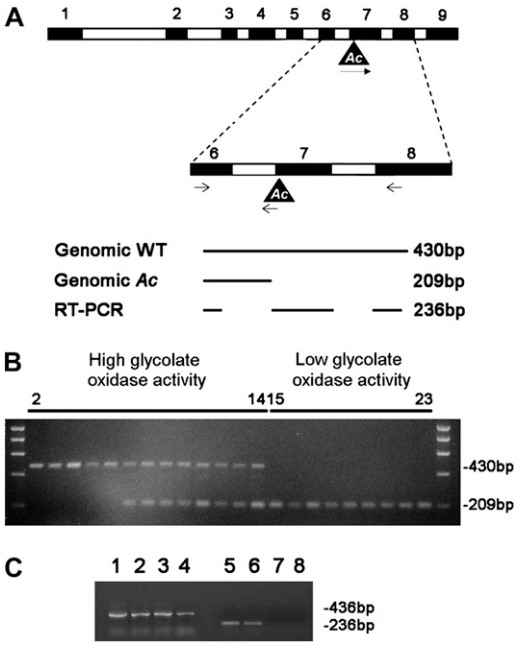

Figure 2. Molecular analysis of the maize *go1*::*Ac* allele. A, Representation of the maize *GO* locus (on BAC clone AC187560.5) and location of the *Ac* insertion. Black boxes signify exons (numbered), while white boxes denote intron sequences. Enlarged region depicts locus from exon 6 through 8 detailing the insertion of an *Ac* element in the beginning of exon 7. Arrows depict oligonucleotide primers in genomic and *Ac*-DNA that amplify wild-type sequences (430-bp fragment) or *Ac*-junction fragments (209 bp). B, Genotypic characterization by PCR analysis of maize seedlings displaying a high or moderate GO activity (lanes 2–14) or low GO activity (lanes 15–23). C, *GO* gene expression. Transcripts from maize seedlings: wild-type (lanes 1 and 5), heterozygote (lanes 2 and 6), or mutant (lanes 3, 4, 7, and 8) seedlings analyzed by reverse transcription-PCR for *GO* expression (lanes 5–8) or actin expression (lanes 1–4). *Ac* transcripts amplify a 436-bp fragment and *GO* transcripts amplify a 236-bp fragment.

enabled us to recover additional sequence information 1 kb upstream and 1 kb downstream of the original *Ac* insertion site. This confirmed that the *Ac* element inserted at the locus was active and enabled us to assemble a contig of approximately 2 kb flanking the *Ac* insertion site.

The *Ac* Insertion Is Located in the *GO1* Locus

Genomic sequences flanking the *Ac* insertion were used to search GenBank and matched genomic DNA (AC187560.5) and mRNA (AY108197). Further BLAST searches indicated the *Ac* insertion was in exon 7 of a putative *GO* gene (Fig. 2A). We reasoned that the mutant phenotype (necrosis and seedling death) was likely caused by accumulation of glycolate and that it may be rescued under high CO_2 conditions where photorespiration is minimal. In an attempt to rescue the seedling lethality of homozygous *go1* mutants, seedlings were grown under high CO_2 conditions (1% to 5% CO_2 in air). Under these conditions, the growth and appearance of the mutants could not be distinguished visually from either the heterozygous or homozygous wild-type individuals (Fig. 3). Seedlings were routinely grown this way for 30 to 60 d. Soon after germination in high CO_2, the phenotype of an individual plant was established using a sensitive GO assay carried out on extracts prepared from discs cut from the first leaf. Later, this phenotype was confirmed on extracts prepared from second or third leaves. As shown in Figure 2B and Table I, seedlings homozygous for the *Ac* insertion allele showed minimal GO activity. Extracts from heterozygous individuals exhibited intermediate capacities to oxidize glycolate (Table I), indicating that a single functional copy of *GO* is insufficient to completely rescue the defect in GO activity. Heterozygote plants appear phenotypically normal, complete a full-life cycle, and are not underrepresented among segregating families. Thus, GO activity of heterozygote individuals is sufficient for plant health in normal air under the growth chamber conditions employed here. Plants with the highest GO activities were homozygous for the functional *GO1* allele (430-bp band in Fig. 2B). As shown in Figure 2C, wild-type plants accumulated *GO* mRNA in contrast to the homozygous mutant plants with the low GO activity, consistent with the

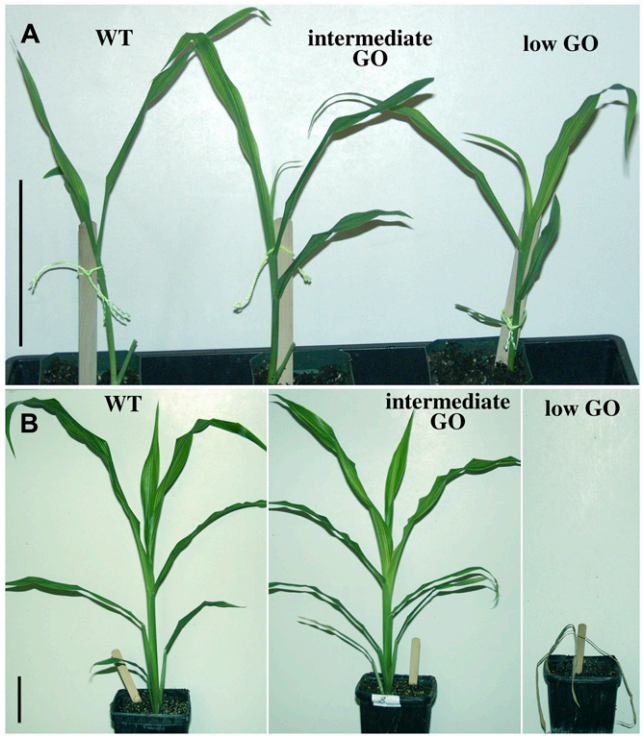

Figure 3. Appearance of maize seedlings with wild-type GO activity (WT), intermediate GO activity, or low GO activity upon transfer from high CO_2 to normal air. The GO activity was 4.44, 2.46, and 0.35 μmol glyoxylate formed (g fresh weight)$^{-1}$ h^{-1} for the three plants, respectively. The size bar on the left represents a height of 18 cm. A, After growth for 14 d in high CO_2 when first transferred to normal air. B, After subsequent growth for a further 15 d in normal air.

severe mutant phenotype of the homozygous insertion. When *go1* mutant seedlings were transferred from high CO_2 to normal air, leaves became necrotic within 7 d, and the seedlings died within 15 d under either growth chamber or greenhouse conditions (Fig. 3B). Taken together these data indicate that the seedling lethality of the mutants is due to the cytotoxic accumulation of glycolate in homozygous individuals due to an *Ac* insertion in the maize *GO1* gene. We therefore named the mutant allele *go1-m1*::*Ac*. A phylogenetic analysis of known GOs from *Oryza sativa* and Arabidopsis reveals two separate protein subgroups (Fig. 4A) in which the maize GO1 (derived from mRNA PCO065133 gb AY108197) is most similar to proteins encoded by Os07g0152900 (91.0%/96.8% identity/similarity) and At3g14415 (83.7%/94.8%; Fig. 4B).

CO_2 Assimilation in Low GO Mutant Is Strongly Inhibited in High O_2

To examine the consequences of the loss of GO activity on *A*, wild-type and *go1* mutant leaf tissue was examined under low (1%) and high (50%) O_2 conditions (Table II). Representative results are shown in Figure 5. Values of *A* attained relatively stable levels after 20 min in high light and low O_2 (Fig. 5). The average value of *A* attained after 40 to 50 min in 1% O_2 was lower for the mutant, but this effect was not statistically significant ($P > 0.05$; Table II). A similar trend was noted for effect of genotype on intrinsic quantum yield of PSII (F_v/F_m in Table II). Though not visible by eye, leaf-to-leaf variation in F_v/F_m was unusually high among mutant leaves, consistent with the occasional occurrence of mild cytotoxic symptoms. An immediate 3% to 4% reduction in *A* occurred upon increasing the O_2 level from 1% to 50% for both genotypes (Fig. 5). During the remainder of the exposure to 50% O_2, the magnitudes of *A* declined on average by 16% (10% in the example illustrated in Fig. 5) for wild type. A similar inhibition of *A* at high O_2 was observed in maize leaves by Dai et al. (1993). In *go1* mutants, *A* declined by an average of 93% (92% in the example given in Fig. 5) relative to high CO_2 conditions. The decline in *A* in the *go1* mutants in 50% O_2 was essentially linear (Fig. 5), and *A* was almost completely abolished after 50 min at this higher O_2 level.

Table I. *Distribution of GO activity in segregating populations of maize plants grown from seeds of selfed mutant heterozygous plants with decreased GO activities*

Plant Material	GO Activity[a]
	μmol glyoxylate formed (g fresh weight)$^{-1}$ *h*$^{-1}$
Low GO	0.66 ± 0.08 (*n* = 39)
Intermediate GO	2.86 ± 0.14 (*n* = 88)
Wild-type GO	6.00 ± 0.30 (*n* = 65)

[a]GO activity was determined on extracts of leaf disks from plants grown in 1% to 5% CO_2 in a chamber in a growth room as described in "Materials and Methods." Samples were taken from 192 plants in seven separate growth experiments. The mean activity values are given ±SE.

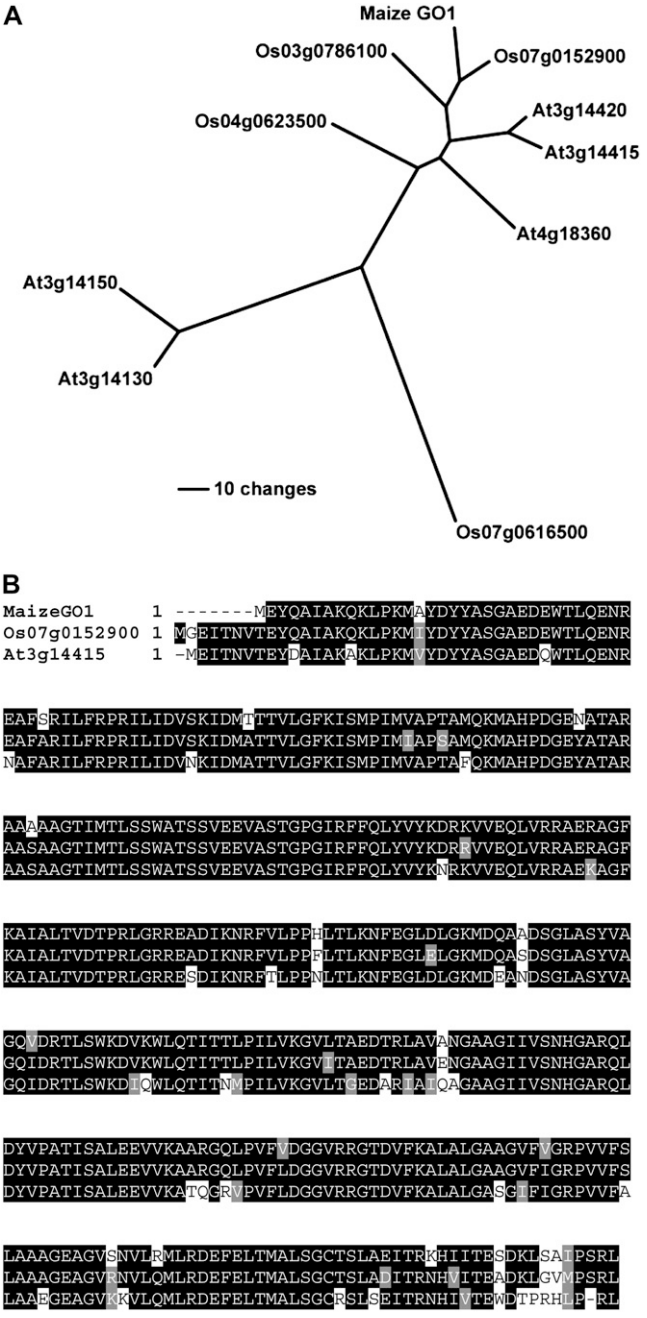

Figure 4. Phylogenetic and amino acid alignment analyses of maize GO1. A, Phylogenetic relationship of maize GO1 with four glycolate oxidases encoded by *Oryza sativa* loci Os07g0152900 (protein ID BAF20823.1), Os03g0786100 (protein ID BAF13401.1), Os04g0623500 (protein ID BAF15839.1), and Os07g0616500 (protein ID BAF22190.1), and with five GOs encoded by Arabidopsis loci At3g14415 (protein ID NP 188059), At3g14420 (protein ID NP 850585), At4g18360 (protein ID NP 193570), At3g14130 (protein ID NNP 188029), and At3g14150 (protein ID NP 188031). The tree represents an unrooted maximum parsimony derived from PAUP 4.0 (Swofford, 2003). B, Alignment of amino acid sequences from maize GO1, Os07g0152900, and At3g14415. Black boxes indicate amino acid identity, gray boxes indicate similar amino acids, and white boxes show no amino acid identity or similarity as determined by ClustalW (Thompson et al., 1994) and Boxshade 3.2.

Table II. *Effects of O_2 on net CO_2 assimilation in wild-type and low GO maize leaves*

Rates of *A* were first measured in 1% O_2 as described in "Materials and Methods." Shown are the initial and final (i.e. 40–50 min later) values of *A* recorded after raising the O_2 level to 50%. Values in parentheses each represent the percent recovery of *A* relative to the preceding rate measurement. The F_v/F_m was measured at the beginning of the experiment after 12 h of dark adaptation. Values are means (±SE) for three replicate leaves.

Parameter	Wild Type	Low GO
A (1% O_2)	9.64 ± 1.28	7.96 ± 0.37
Initial *A* (50% O_2)	8.93 ± 0.89 (96.2% ± 0.3)	7.70 ± 0.37 (96.8% ± 0.6)
Final *A* (50% O_2)	7.91 ± 1.48 (83.9% ± 5.8)[a]	0.54 ± 0.09 (7.0% ± 1.1)
F_v/F_m	0.744 ± 0.004	0.689 ± 0.029

[a]A significant difference due to phenotype based on a T test ($P < 0.05$).

go1 Mutants Do Not Display a General Disruption in the Photorespiratory Cycle

To examine the consequences of a disruption of GO activity on additional reactions of the photorespiratory cycle, *go1* mutants were further characterized by providing [1-^{14}C]glycolate to leaf discs in darkness and measuring the $^{14}CO_2$ produced (Table III). These results are consistent with parallel assays made on leaf extracts showing that *go1* mutants do in fact have a low but measurable activity compared with intermediate and normal plants. An important later step in photorespiration, after oxidation of glycolate, involves the conversion of two Gly to Ser and CO_2 (Fig. 1). Leaf discs taken from *go1* mutants were tested to determine whether any later step in the pathway was also affected by supplying [1-^{14}C]Gly in darkness. Table IV shows that the rate of formation of [^{14}C]Ser and $^{14}CO_2$ was similar for all three genotypes. The mean ratio of CO_2 produced:Ser formed was 1.02, close to the expected stoichiometry, and an ANOVA showed there was no significant difference in the mean ratios among the three genotypes. Thus, plants with low GO activity were not likely altered in their ability to otherwise complete metabolism of photorespiratory Gly.

Glycolate Accumulates in Normal Air in the Low GO Mutant

Though considerable phosphoglycolate is produced by the Rubisco oxygenase reaction, a high GO activity keeps the free glycolate concentration at low steady-state levels in leaves, and even when glycolate concentration increased greatly in short-term experiments in tobacco treated with an inhibitor of GO, the phosphoglycolate concentration was unaffected (Zelitch, 1965). The low concentration of glycolate is likely due solely to the function of GO, as there is no other known mechanism for metabolizing glycolate without it first being converted to glyoxylate. By means of isotope dilution, a glycolate concentration of 0.471 ± 0.038 (SE) μmol/g fresh weight was deduced for maize leaves in light (Jolivet et al., 1985), and by use of HPLC, a value of 1.2 μmol/g fresh weight was obtained (González-Moro et al., 1997). A similar mean steady-state value for wild-type leaves can be obtained from Figure 6 (n = 33) of 0.93 ± 0.12 (SE) μmol glycolate/g fresh weight (1.0 cm^2 leaf area = 14 mg fresh weight).

When seedlings were transferred from growth in high CO_2 to normal air under the same growth conditions, glycolate concentration in the leaves increased rapidly and linearly for at least 6 h in *go1* mutants to a level of 6.3 μmol glycolate/g fresh weight, a 7-fold increase (Fig. 6). After a total of 25 h in air, the glycolate concentration increased to 10.0 μmol glycolate/g fresh weight, an 11-fold increase over the initial concentration. An increase in glycolate concentration in maize leaves induced by photorespiratory inhibitors was accompanied by a decrease in *A* (González-Moro et al., 1997), and a level of 4.0 μmol glycolate/g fresh weight was sufficient to completely abolish *A*. This inhibitory glycolate concentration was reached after about 3 h in normal air in mutant leaves (Fig. 6). The linear increase in glycolate in *go1* mutants (Fig. 6) is consistent with the linear loss of *A* capacity in 50% O_2 and high light (Fig. 5).

DISCUSSION

Consistent with lower rates of oxygenation of ribulose bisphosphate, it has often been noted that in C_4 plants, the enzymes of the photorespiratory pathway,

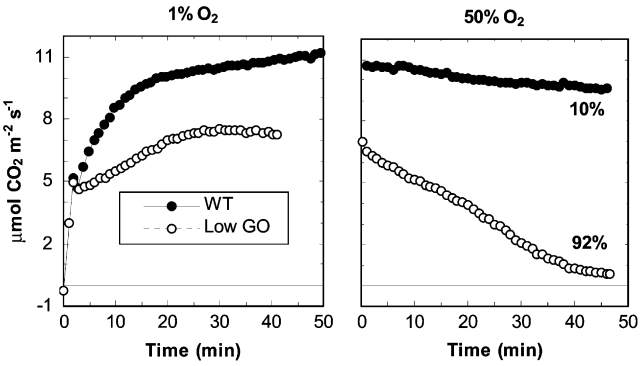

Figure 5. Time course of net CO_2 assimilation in wild-type and *go1* mutant leaves. Dark-adapted leaves were exposed to high light at time zero in a gas phase containing 1% O_2 and subsequently 50% O_2. The percentages in the right panel indicate the extent of loss of *A* at the end relative to the initial exposure to 50% O_2. See "Materials and Methods" for further details.

Table III. *Metabolism of [1-^{14}C]glycolate by maize leaf discs in darkness in a segregating mutant population with varying GO activities*

The mean GO activities assayed from leaf disc extracts are given for each plant material ±SE (n = 5). Enzymatic $^{14}CO_2$ production during the 2-h incubation is likewise reported as the corrected count rate (n = 3).

Plant Material	GO Activity	Enzymic $^{14}CO_2$ Released
	μmol glyoxylate formed (g fresh weight)$^{-1}$ h^{-1}	*dpm*
Low GO	0.19 ± 0.07	252 ± 28
Intermediate GO	3.44 ± 0.60	8,400 ± 2,160
Wild-type GO	5.35 ± 1.00	7,300 ± 3,790

including GO, are present at much lower levels than in C_3 plants (Edwards and Walker, 1983; Dai et al., 1995). For example, the GO specific activity in C_3 grasses is approximately 10-fold greater than in maize (Ueno et al., 2005), and we have also found (I. Zelitch, unpublished data) that on a leaf area basis, maize has about 10% as much GO activity as the C_3 tobacco leaf. Nevertheless, no mutant has previously been described in a C_4 plant in which *GO*, or any other gene underlying an enzymatic step of the photorespiratory pathway, was defective. We have shown here that a homozygous disruption of the *GO1* gene produces a conditional lethal mutation. This mutant is analogous in its phenotype to other mutants that disrupt enzymatic steps in photorespiration, as previously described for Arabidopsis and other C_3 species (Ogren, 1984, 2006) and shows that a functional photorespiratory pathway is essential for maize seedling development.

As shown in Figure 1, glycolate is an early intermediate following the oxygenation of ribulose-1,5-bisphosphate. To examine the effects of glycolate accumulation on carbon assimilation in maize, González-Moro et al. (1997) excised maize leaves in light and supplied them with inhibitors of photorespiratory enzymes. Following the treatments, leaf glycolate concentrations rose from 1.2 μmol/g fresh weight to 4.0 μmol/g fresh weight, at which time CO_2 assimilation was completely blocked, Rubisco activity decreased, and the ribulose bisphosphate concentration increased. They later showed that adding 10 or 20 mM glycolate to excised maize leaves together with low levels (1 mM) of phosphinothricin, an inhibitor of Gln synthetase, greatly increased the inhibitory effect on CO_2 assimilation within several hours (González-Moro et al., 2003). These inhibitory effects were attributed to the higher leaf glycolate concentrations.

Three isoforms of GO have been identified in maize. Two isoforms are localized to the BS, representing 80% of the total activity, and one to the M cells (Popov et al., 2003). Given the restriction of Rubisco to the BS cells, it is perhaps not surprising that the majority of the GO activity is restricted to this compartment. Several lines of evidence support the contention that the majority of this activity is associated with GO1. First, a single lesion at the *GO1* locus eliminates all but 5% to 10% of the activity of wild-type leaves as assayed in leaf extracts (Table I) and shows a low rate of metabolism of [1-^{14}C] glycolate in intact leaf tissue (Table III). Importantly, this residual activity in the mutant is insufficient to prevent rapid accumulation of glycolate in normal air and seedling lethality. Second, molecular analyses correlated genotype with enzymatic phenotype. Plants with intermediate or high GO activities had at least one wild-type *GO1* locus, whereas all plants with low GO activities were homozygous for the *Ac* insertion in the *GO1* locus (Table I; Fig. 2). Third, the maize GO1 is most similar to *Oryza* and Arabidopsis GO enzymes, which are highly expressed in leaves (Fig. 4B). Although we attempted to examine the cell-specific expression of *GO1* in separated BS and M cells, it was not possible to conclusively determine cell-specific expression as the transcript is transcribed at a lower rate or rapidly degraded during the isolation of maize M cell protoplasts (data not shown).

As we have discussed, photorespiration in maize is normally low, but our results confirm that it is not

Table IV. *Metabolism of [1-^{14}C]Gly to $^{14}CO_2$ and [^{14}C]Ser in darkness by maize leaf discs in a segregating mutant population with varying GO activities*

The [^{14}C]Gly and [^{14}C]Ser were separated by HPLC as described in "Materials and Methods." The mean values are given for each plant material ±SE (n = 3).

Plant Material	$^{14}CO_2$ Released	[^{14}C]Ser Formed	$^{14}CO_2$ to [^{14}C]Ser
	dpm		*mean ratio*[a]
Low GO	23,900 ± 2,410	21,300 ± 1,260	1.12
Intermediate GO	22,900 ± 1,730	22,400 ± 2,080	1.02
Wild-type GO	25,000 ± 5,340	29,200 ± 7,510	0.86

[a]One-way ANOVA indicated no significant effect (P = 0.43) of GO phenotype on the $^{14}CO_2$ to [^{14}C]Ser ratio. The mean ratio calculated across all phenotypes was 1.02 (SE ± 0.07; n = 9).

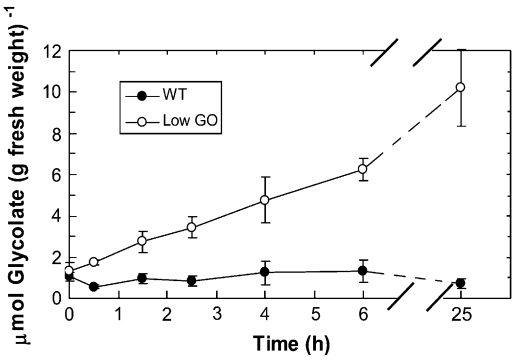

Figure 6. Glycolate levels in wild-type (WT) and low GO maize leaves versus time in light and normal air. Two experiments were conducted with plants after 32 and 21 d of growth in high CO_2, respectively. Three plants with wild-type GO activity and three with low activity were used in one experiment and two different plants with wild-type activity and one with low activity in the second experiment. The mean GO activity as micromoles glyoxylate formed (grams fresh weight)$^{-1}$ hour^{-1} (±SE) for low GO plants was 0.46 ± 0.12 (n = 9) and for wild-type GO plants was 5.92 ± 0.52 (n = 10). The plants were first sampled after 1 h in darkness in normal air and then kept in light for 14 h, in darkness for 6 h, then in light again and leaf samples taken after 5 h. The mean glycolate concentrations are shown (n = 5 for each time point for wild-type GO plants and n = 4 for low GO plants; error bars indicate ±SE).

entirely absent, so we must conclude that the CO_2-concentrating mechanism in the BS cells does not completely suppress Rubisco-catalyzed oxygenation of ribulose bisphosphate, the primary source of glycolate (Figs. 1 and 6).

This conclusion is consistent with previous studies (Dai et al., 1995; González-Moro et al., 1997, 2003) that suggested photorespiration is operational in maize. In 50% O_2 and high light, we also observed that A declined rapidly and linearly with time in the low GO mutant (Table II; Fig. 5). Moreover, and despite residual low levels of GO activity in *GO1* mutants, there are indications of chronic glycolate toxicity even under the high CO_2 conditions used to rescue these mutants. This is not surprising when considered in the context of the Rubisco mechanism (see below). We note the modest tendency toward lower values of A in 1% O_2 and especially F_v/F_m in the mutants (Table II; Fig. 5). The latter is a sensitive indicator of stress. This suggests that even minute traces of glycolate production exert cumulative detrimental effects that become visible only in the later stages.

The reaction catalyzed by GO is the only known route for processing of glycolate. Hence, our results show that accumulation of glycolate is a causal agent leading to inhibition of metabolic processes associated with A in C_4 photosynthesis. The results strongly support the view that an important function of GO and the photorespiratory pathway is the avoidance of buildup of toxic levels of glycolate, as has previously been suggested (González-Moro et al., 1997, 2003). The pattern of necrosis in mutant leaves exposed to normal air does not first appear at the leaf/ligule base where cells display a more C_3-like character, but rather begins at the leaf tip consistent with a persistent requirement for high GO activity throughout leaf development (data not shown). The need to rapidly dispose of glycolate is thus as important to C_4 physiology as it is to C_3 physiology.

The question has often been posed: does photorespiration have a function? There is some evidence that glycolate can strongly inhibit Q_A/Q_B electron transfer by displacement of bicarbonate bound to the non-heme iron in PSII (Petrouleas et al., 1994). However, these authors doubted a physiological role for glycolate based on weak binding of this anion at pH 7.5, a value close to that existing in the stroma. It has often been suggested that photorespiration serves as a sink to dissipate excess reducing power that accumulates under high light conditions (Kozaki and Takeba, 1996). However, it should be pointed out that photorespiration utilizes photochemical energy as does the photosynthetic carbon reduction cycle, so that any interference with either process could potentially cause photoinhibition resulting from overreduction. For example, transgenic tobacco (C_3) plants with decreased activity of the photorespiratory cycle enzyme Gln synthetase were reported to exhibit greater susceptibility to photoinhibition (Kozaki and Takeba, 1996). On the other hand, all higher plants possess an effective array of H^+- and carotenoid-dependent mechanisms to cope with excess light (Ruban et al., 2007; Ahn et al., 2008). Thus, a redundant contribution to photoprotection by such a slow rate of photorespiration as occurs in maize is unlikely to explain the rapid and inescapable lethality of GO deficiency under mild conditions in air.

Ogren (1984) emphasized that the photorespiratory pathway is necessary only when the Rubisco oxygen-

Table V. *Oligonucleotides used in this study*

Oligonucleotide Name	DNA Sequence 5′–3′
AcGO1	ACGGGATTTTCCCATCCTAC
GO 3′UTR F	GATACTCAGCTCGTGCATGGAT
GO 3′UTR R	CAAATACAGAGAGATCACCATGTGC
GOA1	GCCGTCAATGAAACCAAACCAGAGACC
GOA2	GTCCTTGCAGCGGCGTACCATCTGG
GOB1	CTGAATCAGCAGCCTGCCCATG
GOB2	TCGACGAAGCTCCATATGTACTGC
GOC1	AAGTCGACCGCACCCTGAGCTG
GOC2	AGACGTCAAGTGGTTGCAGACCA
GO IN2 F	AACTTCAAGCGTCGAGGAGGTTGC
GO IN2 R	ACCTTCGAAGTTCTTGAGCGTCAG
GO IN3 F	CTGACGCTCAAGAACTTCGAAGGTC
GO IN3 R	TGGTCTGCAACCACTTGACGTC
GO OUT F	ACACCTGACGCTCAAGAACTTCG
GO OUT R	CACTGGAATCGGGGAGCTG
GO OUT R2	GGACATCTGCAGACCATTATGG
GO OUT R3	TGAAGGCAGGGTAACCA
GOP1	CGCTCGCTCTTGGCGCTTCTG
GOP2	CATGTGCAGACAAGGCAGCTCTGG
ZGO1	CACACCTGACGCTCAAGAACT
ZGO2	GTGGTTCGACACGATGATCC

ase reaction occurs. The presence of the photorespiratory pathway is even more imperative insofar as the oxygenase activity of Rubisco is ubiquitous (Jordan and Ogren, 1981) and is, in effect, an intrinsic feature of the interaction of the enzyme with ribulose bisphosphate (Lorimer and Andrews, 1973). Thus, glycolate will inevitably be synthesized if O_2 is present. Regardless of the mechanisms of glycolate toxicity, the necessity of avoiding glycolate accumulation presents sufficient selective pressure to account for the universal presence of the photorespiratory pathway in oxygenic photosynthesis. This is consistent with initial findings demonstrating lethal effects of photorespiratory pathway lesions in Arabidopsis (Ogren, 2006). This article offers strong genetic and biochemical support for the importance of photorespiration in maintaining low (nontoxic) levels of glycolate.

MATERIALS AND METHODS

Ac Mutagenesis and Cloning of GO1

The *go1* mutant was identified in sandbench screens of lines segregating newly transposed *Ac* elements. To identify an *Ac*-containing restriction fragment polymorphism, genomic DNA was fractionated using *Eco*RI and resolved on a 0.8% agarose gel prior to transfer to nylon membranes as previously described (Kolkman et al., 2005). A 3.2-kb *Ac*-containing restriction fragment that cosegregated with the mutant phenotype was identified using the internal 700-bp *Eco*RI/*Hin*dIII fragment of *Ac* as a molecular probe. Inverse PCR reactions were performed using the iPCR-1 protocol as previously described (Kolkman et al., 2005) to amplify an approximately 800 bp of DNA flanking the *Ac* insertion. *Ac* casting reactions were conducted using two rounds of PCR with the *Ac*-specific primers TBp34, TBp35, JGp2, and JGp3 as previously described (Singh et al. 2003). GO-specific primers used include: GO 3′UTR F; GO 3′UTR R; GO OUT F; GO OUT R; GO IN2 F; GO IN2 R; GO OUT R2; GO OUT R3; GOB1; GOB2; GOC1; GOC2; GOA1; GOA2; GOP1; GOP2; GO IN3 F; and GO IN3 R (Table V). Casting products were assembled into a contig using Sequencher Software (Gene Codes Corporation) and used in BLAST searches against maize (*Zea mays*) GSS reads.

Growth of Plants in High CO_2

Plants were grown in an environmental control chamber under an 18-h-light/6-h-dark photoperiod and 250 μmol photons m^{-2} s^{-1} light provided by sodium vapor lamps. The temperature regime was 30°C light/20°C dark. Eight plastic pots (each 2.2 L in volume) were filled with moistened sterile Promix-BX (peat-based medium containing perlite, vermiculite, and limestone), and the pots were placed in a tray containing water. Four seeds of a population segregating for GO activity were placed in each pot. A portable chamber (total gas volume 219 L) covered with clear plastic was placed over the pots and 1% to 5% (v/v) CO_2 in air was continuously pumped into the middle of the chamber at 1 L min^{-1}. Care was taken to avoid simultaneous exposure to actinic light and normal air during plant growth. A complete nutrient solution containing 800 mg L^{-1} nitrogen, Jack's Fertilizer (J.R. Peters Co.), and 7 mg L^{-1} chelated iron was added to each pot weekly, and at the same time the foliage was sprayed with the same nutrient solution containing 200 mg L^{-1} disulfosuccinic acid (Na salt) to "wet" the leaves. After replacing the portable chamber, the pots were flushed with high CO_2 for 2 h in darkness before the lights were turned on again.

GO Assay

Four 0.8-cm discs (2.0 cm^2; 28 mg fresh weight) were cut with a sharp punch in near darkness from a single leaf from plants grown in high CO_2. The discs were transferred to microfuge tubes that were quickly placed in liquid N_2 and then stored at −70°C. Four samples at a time were thawed in an ice bath for the GO assays. A small amount of washed sand was placed in each tube, and 0.8 mL of cold extraction buffer was added (0.05 M potassium phosphate buffer, pH 8.0, containing 1 mM mercaptoethanol). The leaf discs were ground with a plastic pestle and the tubes centrifuged under refrigeration at 16,000*g* for 10 min. The supernatant was used for the enzyme assays.

The reactions were carried out in 12- × 100-mm test tubes on samples from four plants at a time. For each sample, two separate tubes were used, one without glycolate and the other containing the complete reaction mixture. Each tube had 100 μL of extraction buffer, 100 μL cold (freshly prepared) 1.6% phenylhydrazine hydrochloride, 100 μL freshly prepared FMN (4.8 mg 10 mL^{-1}), 300 μL of leaf extract, and water to make the final volume 1.5 mL. The tubes were shaken at 30°C for 10 min, then at 1-min intervals, 50 μL 0.1 M potassium glycolate was added to every other tube and the reaction continued for 20 min. The reaction was stopped by the addition of 500 μL 12 N HCl. Color development of the glyoxylate phenylhydrazone was induced by the addition of 100 μL 8% potassium ferricyanide to each tube (Jameel et al., 1984), and the A_{535} was determined in a spectrophotometer after 3 to 4 min. For each sample, a correction was made for any A_{535} without glycolate. Under these conditions in a 1-cm cuvette, 0.01 μmol of glyoxylate phenylhydrazone gave an A_{535} of 0.186.

Genotype Analysis

Genomic DNA from leaves was prepared according to Dellaporta (1993). RNA isolation was carried out using TRIzol (Invitrogen) and reverse transcription of RNA with a RCM-RACE kit (Ambion) according to the manufacturer's recommendations. The oligonucleotide primers ZGO1 and ZGO2 flank the *Ac* insertion site and amplify a 430-bp DNA fragment from wild-type maize genomic sequences and a 236-bp DNA fragment from reverse transcribed wild-type mRNA. Primers ZGO1 and AcGO1 amplify a 209-bp DNA fragment from genomic sequences corresponding to the *Ac* insertion allele. PCR parameters employed were: 94°C 3 min; (94°C 30 s; 55°C 30 s: 72°C 1 min) 30 times repeated followed by 72°C 7 min.

Metabolism of [1-^{14}C]Glycolate and [1-^{14}C]Gly by Leaf Tissue

Radioactive calcium [1-^{14}C]glycolate was obtained from American Radiolabeled Chemicals. It was dissolved in water and first passed through a column of Dowex 50 (H^+ form, Bio-Rad) and eluted with water. Potassium glycolate (0.1 M) was added to make the final concentration 40 mM. A portion was added to a column of Dowex 1 X8, 100 to 200 mesh, anion-exchange resin (Bio-Rad) 0.7 cm in diameter and 6 cm in height. The column was eluted with 10 mL of water, then with 4 mL of 4 N acetic acid, and these fractions were discarded. Glycolic acid was eluted by collection of the next 10 mL of 4 N acetic acid (Zelitch, 1972). Recovery of glycolic acid was 95% to 98%. Portions of the radioactive glycolic acid were placed in microfuge tubes and concentrated to dryness in a rotary evaporator under vacuum at room temperature to remove the acetic acid.

For metabolic experiments, 12 0.8-cm leaf discs (6.0 cm^2) were cut with a punch from a leaf obtained from plants growing in high CO_2 and previously identified as having wild-type, intermediate, or low GO activity. The discs were floated on water and transferred to 50-mL Erlenmeyer flasks containing center wells. Potassium [1-^{14}C]glycolate (1.0 mL, 40 mM, 2.41 × 10^6 dpm) was added to each flask, and a control flask omitting leaf discs was used in every experiment. A paper wick moistened with 5 M ethanolamine was placed in the centerwell to trap $^{14}CO_2$. The flasks were covered with aluminum foil, closed with a rubber serum stopper, and shaken for 2 h at 20°C. The paper wicks were removed to scintillation vials and the radioactivity determined by scintillation spectrometry.

Experiments on the metabolism of [1-^{14}C]Gly, 7.1 × 106 dpm, were carried out in a similar manner as those with [1-^{14}C]glycolate. At the end of the experiments, the $^{14}CO_2$ was determined as before. The flask was filled with water to dilute the radioactive substrate, and the leaf discs were killed by placing them in a Ten Broeck homogenizer containing 5 mL of boiling 20% ethanol and kept in a boiling water bath for 5 min. The leaf tissue was ground in the homogenizer, centrifuged, the residue washed with water and centrifuged again, and the combined supernatants further analyzed for radioactive metabolites. A portion of each sample was placed on a Dowex-1 acetate column, and the neutral and basic compounds, including Gly and Ser, were eluted with water. A 1.0-mL portion of each sample was concentrated to 400 μL in a rotary evaporator under vacuum, and 50-μL samples were placed on a HPLC cation exchange Na+ column (PRP × 200, 4.2 × 250 mm, Hamilton) and eluted at 30°C with 25% [NaCl:HCl 0.05 m] and 75% water. Ser and Gly eluted separately in this system. Eluates containing each compound were collected in scintillation vials and their radioactivity determined by scintillation spectrometry.

Photosynthesis Measurements

All measurements were conducted using a computer-controlled, dual channel flow-through apparatus previously described (Peterson et al., 2001). The GO phenotypes of the test plants were confirmed by enzyme assay prior to the gas exchange measurements. Plants were first darkened for 12 h to fully reverse photoprotective thermal dissipation processes. Steady-state chlorophyll fluorescence levels (F_o and F_m) were then measured for the dark-adapted leaves using a PAM 101 system equipped with an ED101BL emitter-detector unit (H. Walz). The maximum quantum yield of PSII was estimated as $(F_m - F_o)/F_m$ (= F_v/F_m) after correction of measurements for fluorescence emission from PSI (Peterson et al., 2001). Rates of *A* by attached maize leaves were measured at 360 μL L^{-1} CO_2 and 25°C. Photosynthesis was induced by providing white light from a tungsten-halogen source at an irradiance of 1,290 μmol photons m^{-2} s^{-1}. The increase in *A* was recorded continuously in a gas phase O_2 concentration of 1% (balance N_2) for 40 to 50 min. The O_2 level was then raised to 50%, and recording of *A* continued for a similar time period.

Determination of Glycolate Levels in Leaf Tissue in Normal Air

Plants were grown in high CO_2 under temperature- and light-controlled conditions as described above. Plants were kept in normal air in darkness for 1 h. Leaf segments were cut from a leaf (zero time), and the same light and temperature conditions were then maintained for the plants as before but in normal air. Successive segments (2–6 cm^2) were cut from the same leaf during the time course, and the segments were placed in microfuge tubes and plunged into liquid nitrogen. The tubes were stored at −70°C. Leaf tissue was extracted in boiling 20% ethanol as described above. The samples were ground and the suspension centrifuged for 10 min at 15,000*g* under refrigeration. The residue was suspended in water and centrifuged again. The combined supernatants were added to columns of Dowex-1 X8 acetate, 100 to 200 mesh, anion-exchange resin (Bio-Rad) 0.8 cm in diameter and 6.0 cm in height. The columns were washed with water, elution continued with 4 mL of 4 N acetic acid that was discarded, and the glycolic acid fraction (also known to contain glyceric acid in leaf extracts) was eluted by addition of 10 mL 4 N acetic acid (Zelitch, 1972). A portion (1.0 mL) of the glycolic acid fraction was concentrated to 200 μL in a rotary evaporator under vacuum at room temperature with quantitative recoveries. Isolation and determination of glycolic acid (and its separation from glyceric acid) was carried out on 20-μL samples of the concentrated fraction by HPLC on an anion exclusion column (Supeloge 610H, 7.4 × 300 mm; Supelco) at 40°C with 0.1% v/v H_3PO_4 in water as the eluent.

ACKNOWLEDGMENTS

We thank Martin P.N. Gent for the HPLC analyses, Regan Huntley and Carol Clark for technical assistance, and Gary Brudvig for helpful comments. We also thank Linda Rymarquis who initially characterized *go1* mutant families.

Received August 26, 2008; accepted September 16, 2008; published September 19, 2008.

LITERATURE CITED

Ahn TK, Avenson TJ, Ballottari M, Cheng Y-C, Niyogi KK, Bassi R, Flemming GR (2008) Architecture of a charge-transfer state regulating light harvesting in a plant antenna protein. Science **320:** 794–797

Blackwell RD, Murry AJS, Lea PJ, Kendall AC, Hall NP, Turner JC, Wallsgrove RM (1988) The value of mutants unable to carry out photorespiration. Plant Physiol **16:** 155–176

Bowes G, Ogren WL, Hageman RH (1971) Phosphoglycolate production catalyzed by ribulose diphosphate carboxylase. Biochem Biophys Res Commun **45:** 716–722

Dai Z, Ku M, Edwards GE (1993) C_4 photosynthesis. The CO_2-concentrating mechanism and photorespiration. Plant Physiol **103:** 83–90

Dai Z, Ku MSB, Edwards GE (1995) C_4 photosynthesis. The effects of leaf development on the CO_2-concentrating mechanism and photorespiration in maize. Plant Physiol **107:** 815–825

Dellaporta SL (1993) Plant DNA miniprep and microprep: version 2.1-2.3. *In* M Freeling, V Walbot, eds, The Maize Handbook. Springer-Verlag, New York, pp 522–525

de Veau EJ, Burris JE (1989) Photorespiratory rates in wheat and maize as determined by ^{18}O-labeling. Plant Physiol **90:** 500–511

Edwards GE, Walker DA (1983) Photorespiration. *In* C3, C4: Mechanisms and Cellular and Environmental Regulation of Photosynthesis. University of California Press, Berkeley, CA, pp 368–409

González-Moro B, Lacuesta M, Becerril JM, Gonzálelz-Murua C, Muñoz-Rueda A (1997) Glycolate accumulation causes a decrease of photosynthesis by inhibiting RUBISCO activity in maize. J Plant Physiol **150:** 388–394

González-Moro MB, Loureiro-Beldarrain I, Estavillo JM, Duñabeitia MK, Muñoz-Rueda A, González-Murua C (2003) Effect of photorespiratory C_2 acids on CO_2 assimilation, PSII photochemistry and xanthophyll cycle in maize. Photosynth Res **78:** 161–173

Hanson KR, Peterson RB (1986) Regulation of photorespiration in leaves: evidence that the fraction of ribulose bisphosphate oxygenated is conserved and stoichiometry fluctuates. Arch Biochem Biophys **246:** 332–346

Hatch MD (1971) The C_4 pathway of photosynthesis. Evidence for an intermediate pool of carbon dioxide and the identity of the donor C_4-dicarboxylic acid. Biochem J **125:** 425–432

Jameel S, El-Gult T, McFadden BA (1984) Isolation and properties of watermelon isocitrate lyase. Phytochem **23:** 2753–2759

Jenkins CLD, Furbank RT, Hatch MD (1989) Mechanism of C_4 photosynthesis. A model describing the inorganic carbon pool in bundle sheath cells. Plant Physiol **91:** 1372–1381

Jolivet P, Gans P, Triantaphylides C (1985) Determination of glycolic acid levels in higher plants during photorespiration by stable isotope dilution mass spectrometry with double-labeling experiments. Anal Biochem **147:** 86–91

Jordan DB, Ogren WL (1981) Species variation in the specificity of ribulose bisphosphate carboxylase/oxygenase. Nature **291:** 513–515

Kolkman JM, Conrad LJ, Farmer PR, Hardeman K, Ahern KR, Lewis PE, Sawers RJH, Lebejko S, Chomet P, Brutnell TP (2005) Distribution of *Activator* (*Ac*) throughout the maize genome for use in regional mutagenesis. Genetics **169:** 981–995

Kozaki A, Takeba G (1996) Photorespiration protects C3 plants from photooxidation. Nature **384:** 557–560

Laisk A, Edwards GE (1998) Oxygen and electron flow in C_4 photosynthesis: Mehler reaction, photorespiration and CO_2 concentration in the bundle sheath. Planta **205:** 632–645

Lorimer GH, Andrews TJ (1973) Plant photoprotection: an inevitable consequence of the existence of atmospheric oxygen. Nature **243:** 359–360

McHale NA, Havir EA, Zelitch I (1988) A mutant of *Nicotiana sylvestris* deficient in serine glyoxylate aminotransferase activity. Callus induction and photorespiratory toxicity in regenerated plants. Theor Appl Genet **76:** 71–75

Ogren WL (1984) Photorespiration: pathways, regulation, and modification. Annu Rev Plant Physiol **35:** 415–442

Ogren WL (2006) Affixing the O of rubisco: discovering the source of photorespiratory glycolate and its regulation. Photosynth Res **76:** 53–63

Peterson RB (1983) Estimation of photorespiration based on the initial rate of postillumination CO_2 release. II. Effects of O_2, CO_2 and temperature. Plant Physiol **73:** 983–987

Peterson RB, Oja V, Laisk A (2001) Chlorophyll fluorescence at 680 and 730 nm and leaf photosynthesis. Photosynth Res **70:** 185–196

Petrouleas V, Deligiannakis Y, Diner BA (1994) Binding of carboxylate anions at the non-heme Fe(II) of PSII. II. Competition with bicarbonate and effects on the Q_A/Q_B electron transfer rate. Biochim Biophys Acta **1188:** 271–277

Popov VN, Dmitrieva EA, Eprintsev AT, Igamberdiev AV (2003) Glycolate oxidase isoforms are distributed between the bundle sheath and mesophyll tissues of maize leaves. J Plant Physiol **160:** 851–857

Reumann S, Weber APM (2006) Plant peroxisomes respire in the light: some gaps of the photorespiratory C_2 cycle have become filled-others remain. Biochim Biophys Acta **1763:** 1496–1510

Ruban AV, Berera R, Ilioaia C, van Stokkum IHM, Kennis JYM, Pascal AA, van Amerongen H, Robert B, Horton P, van Grondelle R (2007) Identification of a mechanism of photoprotective energy dissipation in higher plants. Nature **450:** 575–578

Singh M, Lewis PE, Hardeman K, Bai L, Rose JKC, Mazourek M, Chomet P, Brutnell TP (2003) Activator mutagenesis of the Pink scutellum1/viviparous7 locus of maize. Plant Cell **15:** 874–884

Swofford DL (2003) PAUP*. Phylogenetic Analysis Using Parsimony (*and Other Methods), Version 4. Sinauer Associates, Sunderland, MA

Thompson JD, Higgins DG, Gibson TJ (1994) CLUSTAL W: improving the sensitivity of progressive multiple sequence alignment through sequence weighting, position-specific gap penalties and weight matrix choice. Nucleic Acids Res **22:** 4673–4680

Tolbert NE (1971) Microbodies: peroxisomes and glyoxysomes. Annu Rev Plant Physiol **22:** 45–74

Tolbert NE (1997) The C_2 oxidative photosynthetic carbon cycle. Annu Rev Plant Physiol Plant Mol Biol **48:** 1–25

Ueno O, Yashimura Y, Sentoku N (2005) Variation in the activity of some enzymes of photorespiratory metabolism in C_4 grasses. Ann Bot (Lond) **96:** 863–869

Usuda H, Edwards GE (1980) Localization of glycerate kinase and some enzymes for sucrose synthesis in C_3 and C_4 plants. Plant Physiol **65:** 1017–1022

Volk RJ, Jackson WA (1972) Photorespiratory phenomena in maize oxygen uptake, isotope discrimination, and carbon dioxide efflux. Plant Physiol **49:** 218–223

Yamaguchi K, Nishimura M (2000) Reduction to below threshold levels of glycolate oxidase activities in transgenic tobacco enhances photoinhibition during irradiation. Plant Cell Physiol **41:** 1397–1406

Zelitch I (1965) The relation of glycolic acid synthesis to the primary photosynthetic carboxylation reaction in leaves. J Biol Chem **240:** 1869–1876

Zelitch I (1972) The photooxidation of glyoxylate by envelope-free spinach chloroplasts and its relation to photorespiration. Arch Biochem Biophys **150:** 698–707

Zelitch I (1973) Alternate pathways of glycolate synthesis in tobacco and maize and its relation to rates of photorespiration. Plant Physiol **51:** 299–305

Zelitch I (2001) Travels in a world of small science. Photosynth Res **67:** 157–176

Zelitch I, Ochoa S (1953) Oxidation and reduction of glycolic and glyoxylic acid in plants. I. Glycolic acid oxidase. J Biol Chem **201:** 707–718